Transmission-Distribution Dynamic Co-simulation of Electric Vehicles Providing Grid Frequency Response

Yijing Liu, Thomas J. Overbye
Texas A&M University
College Station, TX, USA
{yiji21, overbye}@tamu.edu

Wenbo Wang, Xin Fang
National Renewable Energy Laboratory
Golden, CO, USA
{Wenbo.Wang, Xin.Fang}@nrel.gov

Jinning Wang, Hantao Cui, Fangxing Li
University of Tennessee
Knoxville, TN, USA
{jwang175, hcui7, fli}@utk.edu

2022 IEEE Power & Energy Society General Meeting (PESGM) | 978-1-6654-0823-3/22/$31.00 USG | DOI: 10.1109/PESGM48719.2022.9917027

***Abstract*—This paper investigates the impacts of electric vehicles (EVs) on power system frequency regulation based on an open-source transmission-and-distribution (T&D) dynamic co-simulation framework. The development of an EV dynamic model based on an Western Electricity Coordinating Council dynamic model is introduced first, then the T&D dynamic co-simulation platform is described. The advantage of the overall platform is that distributed energy resources, such as distributed photovoltaics and EVs, are modeled explicitly in both transmission and distribution simulators for frequency and voltage dynamics, respectively. The case studies simulate the frequency responses (i.e., primary and/or secondary) of the EVs after the system is exposed to an N-1 contingency, such as a generation trip. Various EV frequency regulation participation strategies are also investigated to study their impacts on system frequency response. The studies shows that EVs have the potential capability to provide effective frequency regulation services.**

***Index Terms*—Electric vehicle, frequency regulation, transmission-and-distribution dynamic co-simulation**

I. Introduction

Many countries have set goals toward or are planning to reach a carbon emissions-free power sector and to reduce carbon emissions of the transportation sector during the next two decades. As a result, an increasing number of electric vehicles (EVs) and charging infrastructure will be deployed in the transmission and distribution networks. Because inverter-based resources—such as EVs, distributed photovoltaics (DPV), and energy storage—are connected to the grid through power electronic devices, the total inertia of the system is decreasing and making the system more vulnerable to frequency fluctuations [1]. Different control strategies for the generation units and storage can be adopted to restore the frequency response by providing real power support [2, 3]. These frequency regulation services, including both primary frequency response (PFR) and secondary frequency response (SFR) [4], can balance the system total load and generation.

EVs, equipped with a battery, have the capability and flexibility to provide fast frequency response, including PFR and SFR, to help mitigate system frequency fluctuations and to enhance system frequency stability; however, this vehicle-to-grid (V2G) frequency regulation provision may impact both the bulk power system frequency response and the local distribution network voltage profiles. Because the charging infrastructure is usually designed to sustain charging of EVs at the rated power, the V2G discharging for frequency regulation could increase local voltage and lead to overvoltage violations.

To synthetically study the impacts of the EVs' frequency regulation on both the bulk power system and a distribution network, this paper leverages a transmission-and-distribution (T&D) dynamic co-simulation model that can simultaneously perform the bulk system dynamic simulation and distribution power flow analysis. The coordination between EVs and other DERs, such as DPV, for frequency regulation is studied. Multiple participation strategies for the frequency response from EVs are investigated. The main contributions of this paper can be summarized as follows:

- An innovative EV dynamic model considering EV owners' participation willingness has been developed and added to the T&D dynamic co-simulation model [4] to enable the analysis of the frequency response from EVs.
- The coordination between the EV and DPV frequency regulation is studied, which provides guidance for future coordination optimization of DER grid services.
- The impacts of EV frequency regulation are analyzed, including PFR and SFR on bulk system frequency response and distribution voltage. Multiple participation strategies of the frequency response from EVs are investigated.

II. EV Model and Simulation Framework

A. EV Model

Plug-in EVs have promising capabilities to provide several T&D grid services [5]. Because EVs are essentially inverter-based resources, we developed an EV dynamic model based on the Western Electricity Coordinating Council PVD1 model [6]. Here, we added 1) a parameter $Pcap$ that models the participation strategies of EV; 2) the state-of-charge (SOC) related blocks that decide the current flowing in and out of the battery, as shown in Fig. 1. Note that a generic model of PFR is also included in Fig. 1. The overall dynamic model can represent general EV battery behaviors, which is added to ANDES [7], a grid electro-mechanical dynamics tool.

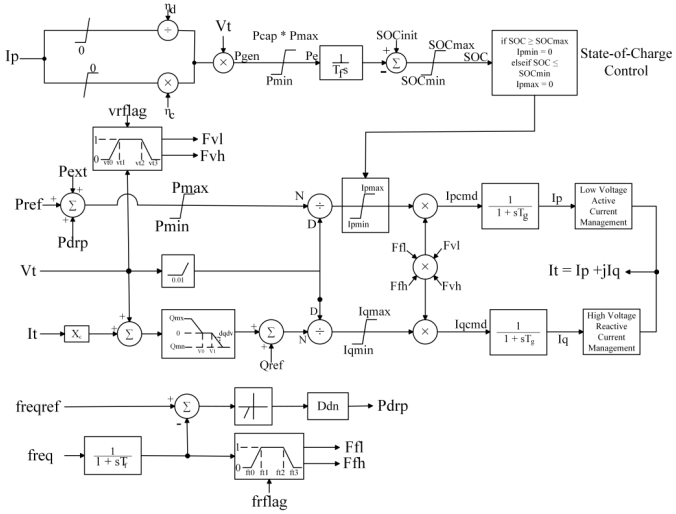

Fig. 1: Block diagram for the EV dynamic model including PFR.

More specifically, *pcap* added in this model limits the participation of an EV to provide frequency regulation. *pcap* is in range [-1, 1], and the meanings of representative values are explained here. When *pcap* =-1, the EV's maximum power is 100% charging, which means that the EV cannot provide PFR and SFR. *pcap* =1 means that the EV's maximum power is 100% discharging, and the EV can change its status from charging to discharging to provide PFR and SFR. Similarly, *pcap* =-0.5 and 0.5 mean that the EV's maximum power is 50% charging and 50% discharging, respectively. *pcap* =0 represents that the EV's maximum power is 0, which means that the EV is not charging or discharging.

a) PFR: PFR uses droop control, i.e., when the frequency deviation is larger than a PFR deadband, the EV changes its active power output accordingly. An additional power output, P_{drp}, is added to the generation output:

$$P_{drp} = \begin{cases} \frac{(60-db_{UF})-f}{60} D_{dn} & \text{if } f < 60 \\ \frac{f-(60+db_{OF})}{60} D_{dn} & \text{if } f > 60 \end{cases} \quad (1)$$

where db_{UF} and db_{OF} are the underfrequency and overfrequency deadband, respectively; and D_{dn} is the per-unit power output change to 1-p.u. frequency change (frequency droop gain).

b) SFR: SFR [8] is enabled by an automatic generation control (AGC) model that includes two components: an area-level (assuming one area in this paper) estimation of the area control error (ACE) and a plant-level control that receives the SFR reference power, P_{ext}, for each plant. ACE represents the system generation and load imbalance. ACE is calculated as:

$$ACE_{tt} = 10B(f_{reqm,tt} - f_0) \quad (2)$$

where tt is the AGC time interval index; ACE_{tt} is the ACE at the AGC interval tt; $f_{reqm,tt}$ is the measured system frequency at the AGC interval tt; f_0 is the system reference frequency; and B is the frequency bias in $MW/0.1Hz$. After a frequency error tolerance deadband, f_{db}, a proportional-integral (PI) control is applied on the ACE signal to calculate

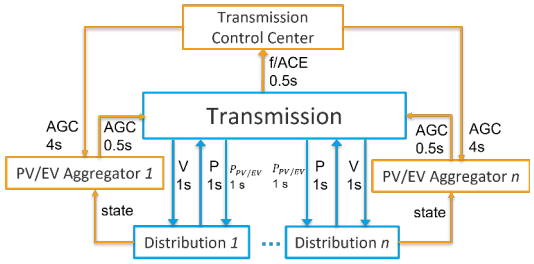

Fig. 2: Simulation components with information exchange

the control variable, $u(t)$ (i.e., AGC signal); K_P and K_I are the coefficients of the AGC PI controller:

$$u(t) = -K_P ACE - K_I \int ACE. \quad (3)$$

The AGC signals are normally updated every 4 s in the field. The output from the PI controller is allocated to each AGC generator considering the unit's participation factor, resulting in the final AGC control reference for each unit. Note that the participation factor of each unit is decided by a real-time economic dispatch that is normally updated every 5 minutes. Each EV's participation factor can be updated by the corresponding EV aggregator and/or under a different time interval based on the local aggregator's optimization.

B. T&D Dynamic Co-simulation Platform

This section introduces the T&D dynamic co-simulation framework for studying effect of EVs on frequency response. The backbone of this framework is developed in [4]. The co-simulation framework is based on the HELICS platform and the open-source power system simulator ANDES and OpenDSS [9]. HELICS is an open-source, cyber-physical co-simulation framework for energy systems. Following are a few key concepts of HELICS that are relevant here: federates, brokers, simulators, and messages; for more details, see [10].

The developed EV component enables EV frequency response studies (see Section II). Assume that the overall system comprises a transmission system; a control center; and an EV aggregator and a photovoltaic (PV) aggregator for each load bus, as shown in Fig. 2. The transmission system sends the system frequency and the ACE signals to the transmission control center every 0.5 second, where the AGC signals are calculated with the PI controller and sent to the EV and PV aggregators every 4 seconds. This setup is modeled in HELICS, where the transmission simulation federate uses ANDES, and the distribution quasi-static time-series power flow uses OpenDSS.

III. Case Studies

This section illustrates the V2G impacts on frequency response by T&D co-simulation. Two sets of cases are studied. Case set 1 explores the impact of DPV and EVs on frequency response. Case set 2 tests various EV participation strategies to analyze their effects on system frequency response.

978-1-6654-0823-3/22/$31.00 ©2022 IEEE

A. Overview of the Large-Scale T&D Test System

Fig. 3 (a) shows a one-line diagram of the transmission system. This is a 2000-bus model and there are 10 different voltage levels. Approximately 67 GW and 19.4 GVAr of load are served by 544 generators of various fuel types, with approximately 98 GW of installed capacity. The transmission case can be found in [11], and the original data is in PSS/E format for the power flow (raw file) and dynamics (dyr file) data [12, 13]. Since some dynamic models in the original PSS/E data set are not supported by ANDES, a database conversion tool is developed. The unsupported dynamic models in the original case are converted to functionally similar and supported models in ANDES. The differences of frequency profiles after selected N - 1 contingency events stays below 10% comparing to the original case. Conversion details are not discussed here since the purpose of this work is analyzing V2G impact on frequency response, rather than reproducing the original case. The power flow and dynamics data are parsed using a built-in tool in ANDES and then fed into ANDES. The transmission network is tested in ANDES to ensure that the case can be initialized properly and has a flat start.

The distribution system covers the geographic area of Austin, Texas, and consists of six subregions [14]. The 243 distribution feeders in the five urban regions replace approximately 2.83 GW of load in the transmission system. A load total of 360k and more than 1 million electrical nodes are simulated in the distribution system. There are 8400 DPV units and 42,000 EVs connected to distribution feeders (200 DPV units and 1000 EVs at each of 36 substations and 400 DPV units and 2000 EVs at each of the remaining three substations). Each EV is assumed to have a rated power of 7 kW [15] and a rated energy of 50 kWh. The assumed EV rated power of 7 kW is taken from [15], most electric vehicles charging at home on a 240-volt level 2 charger will draw about 7,200 watts or less. The total DPV power output is 222.7 MW, and the total installed DPV capacity is 2.1 GW. All 42,000 EVs consume 294 MW (charging at rated power) of power, and the total frequency regulation headroom is 588 MW (from rated charging to discharging). The co-simulation is performed on a high-performance computer, Eagle, at National Renewable Energy Laboratory. The simulations assume that at the 10th second, a generator in the Austin area, with 477 MW of real power output, is dropped. The SFR is provided only by the connected DPV and EVs in the system.

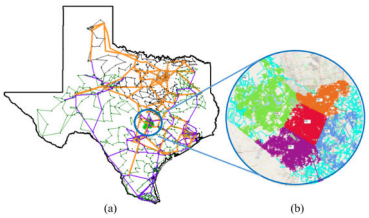

Fig. 3: (a) One-line diagram of the 2000-bus case [11, 12], with Austin area colored in green and (b) five urban subregions in the distribution Austin data set [16]

B. Comparison between DPV and EV Frequency Regulation

This subsection explores the impacts of DPV and EVs on balancing generation and demand. Both PFR and SFR are considered. Details of each scenario are given in Table I. In Case 1_1, DPV and EVs do not provide SFR (AGC). In Case 1_2, only DPV provides SFR, and it's the opposite in Case 1_3. In Case 1_4, both DPV and EVs provide SFR to the grid.

TABLE I: DETAILS OF FOUR SCENARIOS

	Case 1_1	Case 1_2	Case 1_3	Case 1_4
DPV AGC	off	on	off	on
EV AGC	off	off	on	on

Fig. 4 shows the system frequency response after the generation trip event under the four cases. The system frequency drops immediately when the event happens, and it starts to recover soon afterward, with PFR from both conventional units and DERs (i.e., DPV and EVs). Without DERs providing SFR (Case 1_1), the system frequency cannot return to 60 Hz because in this testing system, conventional generators do not provide SFR. In both Case 1_2 and Case 1_3, the headroom of the DPV and EVs, respectively, are enough to cover the amount of generation loss, such that the frequency can be restored to 60 Hz after approximately 100 seconds. The frequency response curves of Case 1_2 and Case 1_3 are quite close because the dynamic parameters (droop parameters and inverter settings) of the EVs and DPV are the same. When both DPV and EVs provide SFR (Case 1_4), the system can recover, and the frequency recovery process is shorter.

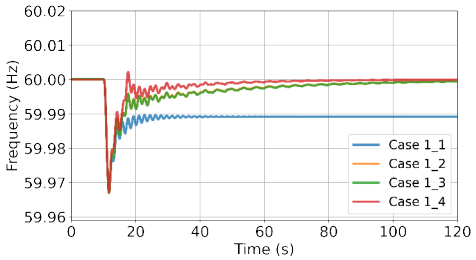

Fig. 4: System frequency response under different scenarios

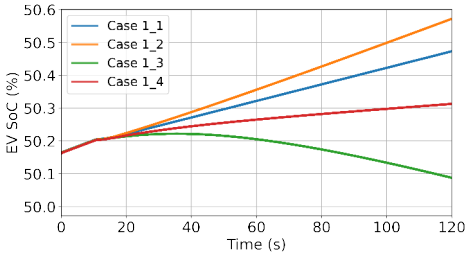

Fig. 5: EV SOC under different scenarios

Fig. 5 demonstrates the impacts of EV frequency regulation provision on its battery SOC. The EVs are constantly fully charging before the event. After the contingency, PFR is activated first, and SFR increases the power output of the EVs after receiving the AGC signal. As shown in the results from cases 1_1 and 1_2 (EV AGC off) and from cases 1_3 and 1_4 (EV AGC on), the EV charging patterns are all different

978-1-6654-0823-3/22/$31.00 ©2022 IEEE

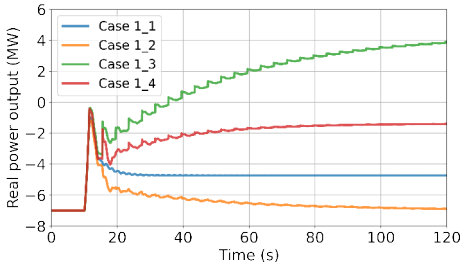

Fig. 6: EV real power output under different scenarios

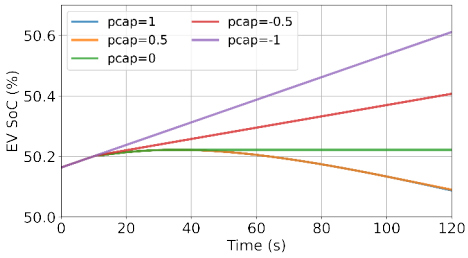

Fig. 8: EV SOC under five frequency regulation strategies

despite the same EV AGC settings. The interactions between the system and the EVs change the charging speed of the EVs, as shown in Fig. 6. More specifically, the EV charging speed is different in cases 1_1 and 1_2. In Case 1_1, since the system frequency cannot be restored to 60 Hz, the PFR of the EVs will be activated, and the EVs provide PFR to support the frequency during the whole simulation horizon; therefore, the EVs will not be fully charging in this case even when the frequency is stable, as shown in Fig. 6. In Case 1_2, with the SFR support from the DPV, the system frequency can be restored to 60 Hz, and PFR of the EVs will phase out once the frequency is restored; therefore, the power output of the EVs will be restored to fully charging once the frequency is restored to 60 Hz, as shown in Fig. 6. In Case 1_3, the burden on the EVs is heavier (with only EVs providing SFR) compared with Case 1_4, when both DPV and EVs provide SFR, so they starts to discharge; therefore, the EVs start to discharge in Case 1_3. Consequently, the SOC of the EVs is the lowest in Case 1_3, when only the EVs provide SFR. The SOC of the EVs will be the highest in Case 1_2, when they do not provide SFR and the PFR reduces to 0. The EV power consumption varies as the EV and DPV frequency support strategies change. The SFR settings of both the EVs and DPV impact the charging pattern of the EVs.

C. Impacts of EV Participation Factor

This subsection investigates the impacts of different EV frequency regulation strategies. Five EV frequency regulation strategies have been tested with varying *pcap* values (i.e., -1, -0.5, 0, 0.5, 1), as discussed in Subsection II.A. The AGC signal is disabled for DPV, so they do not provide any SFR.

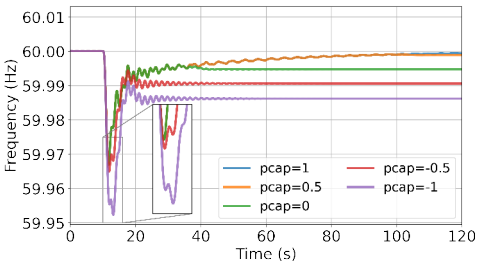

Fig. 7: Frequency response under five frequency regulation strategies

When *pcap* = -1 (the violet line in Figs. 7–9), the EVs do not have headroom for both PFR and SFR. The maximum power output of the EVs is 100% charging all the time. The EVs participate in neither PFR nor SFR. The EV charging rate is constant 100% all the time. Under this situation, the frequency nadir after the generation drop event is lower than Case 1_1 in Case set I because the EVs cannot provide PFR with *pcap* = -1, and the system frequency cannot return to 60 Hz. In Case 1_1, however, the EV can still provide PFR without providing SFR.

When *pcap* = -0.5 (the red line), the maximum power output of the EVs is set to be 50% charging. The frequency nadir is higher than that when *pcap* = -1 because the EVs have 50% charging power headroom to provide PFR after the contingency with *pcap* = -0.5. But the nadir is lower than in the other scenarios because the PFR provided by the power headroom of the EVs is limited by the *pcap* value.

The scenario with *pcap* = 0 (the green line) is an edge case. The charging rate of the EVs starts to decrease to 0 after the loss of generation. Starting from $pcap \geq 0$, the amount of PFR power support is no longer limited by the EV headroom but by the droop parameters, and the frequency nadirs are almost the same since the droop parameters of the EVs are the same.

When $pcap > 0$ (the blue & the orange lines), the EVs can send power to the grid. After the contingency, the real power output increases (from charging to discharging), the SOC of the EVs decreases, and the system frequency gradually recovers. Note that there is only a slight difference when *pcap* changes from 0.5 to 1 after 100 seconds for the three curves including the system frequency response, the EV SOC, and and the EV power output. This is because the total amount of power support from the PFR and SFR by the EVs with *pcap* = 0.5 are nearly enough to cover the power imbalance.

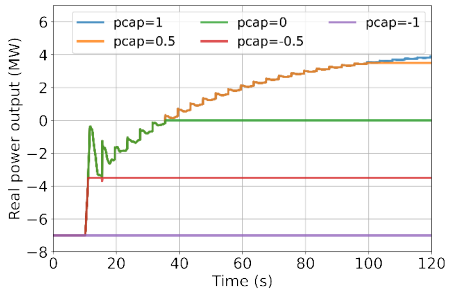

Fig. 9: EV power output under five frequency regulation strategies

Fig. 10 shows the voltage profiles of a substation bus and all downstream feeder nodes. It shows the average voltage and the three-sigma (standard deviation) range of the voltage that covers 99% of the feeder's nodes. One can observe that the voltage increases and then decreases after the generation

978-1-6654-0823-3/22/$31.00 ©2022 IEEE

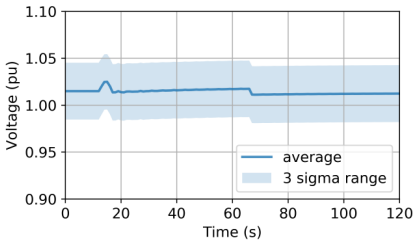

Fig. 10: Case $pcap = 1$: voltage of substation Bus 6032 with all downstream feeders, with medium-voltage and low-voltage nodes

decreases because the local EVs/DPV participate in PFR and SFR. This demonstrates that the co-simulation model can capture the local voltage response.

The simulation results demonstrate that the system conditions, the DER AGC settings, and the EV charging strategies all affect the system frequency response after contingencies. The proliferation of DERs, DPV, and EVs is crucial to the system frequency response, especially in future power systems.

IV. Conclusion

With the increasing electrification of the transportation sector, the impact of EVs on the system frequency stability should be investigated. This paper studies the impact of EVs on the system frequency regulation through a T&D dynamic co-simulation model. Both the PFR and SFR of EVs are studied. Simulation results demonstrate that the aggregation of EVs has great potential to provide both PFR and SFR to restore the system frequency faster after contingencies. Several factors impact the frequency regulation from EVs, such as the participation factor and the potential SOC limits. When EVs are enabled to change their status from fully charging to fully discharging, their capability and flexibility to provide frequency regulation are the largest, and the system frequency can be restored the fastest. While results presented in this paper are based on several assumptions, the outcomes can still reveal EV impact on frequency response using T&D co-simulation platform. Future work includes research on the coordination between EV charging scheduling and frequency regulation to maintain a better trade-off of the system frequency stability and the charging time of the EVs. Sensitivity analysis of *pcap* values will be provided in the future work as well.

Acknowledgments

This work was authored in part by the National Renewable Energy Laboratory, operated by Alliance for Sustainable Energy, LLC, for the U.S. Department of Energy (DOE) under Contract No. DE-AC36-08GO28308. Funding provided by U.S. Department of Energy Office of Electricity Advanced Grid Research and Development program. The U.S. Government retains and the publisher, by accepting the article for publication, acknowledges that the U.S. Government retains a nonexclusive, paid-up, irrevocable,worldwide license to publish or reproduce the published form of this work,or allow others to do so, for U.S. Government purposes. The views expressed in the article do not necessarily represent the views of the DOE or the U.S.Government.

This research was performed using computational resources sponsored by the Department of Energy's Office of Energy Efficiency and Renewable Energy and located at the National Renewable Energy Laboratory.

References

[1] G. Delille, B. Francois, and G. Malarange, "Dynamic frequency control support by energy storage to reduce the impact of wind and solar generation on isolated power system's inertia," *IEEE Trans. Sustainable Energy*, vol. 3, pp. 931–939, 2012.

[2] Y. Liu, Z. Mao, H. Li, K. S. Shetye, and T. J. Overbye, "Integration of renewable generators in synthetic electric grids for dynamic analysis," *arXiv preprint arXiv:2101.02319*, 2021.

[3] X. Fang, H. Yuan, and J. Tan, "Secondary frequency regulation from variable generation through uncertainty decomposition: An economic and reliability perspective," *IEEE Trans. Sustainable Energy*, 2021.

[4] W. Wang, X. Fang, H. Cui, F. Li, Y. Liu, and T. J. Overbye, "Transmission-and-distribution dynamic co-simulation framework for distributed energy resource frequency response," *IEEE Transactions on Smart Grid*, 2021.

[5] V. V. Viswanathan and M. Kintner-Meyer, "Second use of transportation batteries: Maximizing the value of batteries for transportation and grid services," *IEEE Trans. Vehicular Technology*, vol. 60, no. 7, pp. 2963–2970, 2011.

[6] "Generic Models (PV Plants)". [Online]. Available: https://www.esig.energy/wiki-main-page/generic-models-pv-plants/

[7] H. Cui, F. Li, and K. Tomsovic, "Hybrid symbolic-numeric framework for power system modeling and analysis," *IEEE Trans. Power Systems*, vol. 36, no. 2, 2020.

[8] W. Wang, X. Fang, and A. Florita, "Impact of DER communication delay in agc: Cyber-physical dynamic co-simulation," in *IEEE 48th Photovoltaic Specialists Conference (PVSC)*, 2021, pp. 2616–2620.

[9] R. C. Dugan and T. E. McDermott, "An open source platform for collaborating on smart grid research," in *2011 IEEE Power and Energy Society General Meeting*, 2011, pp. 1–7.

[10] B. Palmintier, D. Krishnamurthy, P. Top, and et al, "Design of the helics high-performance transmission-distribution-communication-market co-simulation framework," in *2017 Workshop on MSCPES*. IEEE, 2017, pp. 1–6.

[11] "Electric Grid Test Case Repository". [Online]. Available: https://electricgrids.engr.tamu.edu/

[12] A. B. Birchfield, T. Xu, K. M. Gegner, K. S. Shetye, and T. J. Overbye, "Grid structural characteristics as validation criteria for synthetic networks," *IEEE Trans. Power Systems*, vol. 32, no. 4, pp. 3258–3265, 2017.

[13] T. Xu, A. B. Birchfield, and T. J. Overbye, "Modeling, tuning, and validating system dynamics in synthetic electric grids," *IEEE Trans. Power Systems*, vol. 33, no. 6, Nov. 2018.

[14] H. Li, J. L. Wert, A. B. Birchfield, T. J. Overbye, T. G. S. Roman, C. M. Domingo, F. E. P. Marcos, P. D. Martinez, T. Elgindy, and B. Palmintier, "Building highly detailed synthetic electric grid data sets for combined transmission and distribution systems," *IEEE OAJPE*, vol. 7, pp. 478–488, 2020.

[15] "Electric Vehicle Charging at Home Typically Draws Less Than Half the Power of an Electric Furnace". [Online]. Available: https://www.energy.gov/eere/vehicles/articles/fact-995-september-18-2017-electric-vehicle-charging-home-typically-draws

[16] N. Panossian, T. Elgindy, B. Palmintier, and D. Wallison, "Synthetic, realistic transmission and distribution co-simulation for voltage control benchmarking," in *2021 IEEE Texas Power and Energy Conference (TPEC)*. IEEE, 2021, pp. 1–5.